

ERL2011 SUMMARY OF WORKING GROUP 2 BEAM DYNAMICS

C. Mayes, Cornell University, Ithaca, NY 14853, USA
N. Nakamura, KEK Tsukuba, Ibaraki 305-0801, Japan

Abstract

The 50th ICFA Advanced Beam Dynamic Workshop on Energy Recovery Linacs (ERL2011) was held on October 16-21, 2011 at KEK in Japan. Five working groups, Working Groups 1- 5, were organized in the workshop and Working Group 2 mainly covered topics and issues of beam dynamics for ERLs. This paper summarizes WG2 presentations and activities.

INTRODUCTION

The number of existing and future ERL based accelerator projects are steadily increasing in North America, Europe, and Asia. In ERL2011, Working Group 2 (WG2) surveyed the optics designs of nearly all of these machines, and included operational experiences at existing machines. WG2 also addressed the critical issues of collective effects, beam instabilities, start to end simulation, simulation codes, halo formation, etc. in order to realize the excellent ERL performance such as ultra-low emittance bunches, ultra-short bunches, and high current.

There were 7 WG2 sessions in which 28 oral presentations were presented in total. The presentation time was set to 20 or 25 minutes including a 5-minute question time. Two of the sessions were held as joint sessions with Working Groups 1 (Electron Sources) and 5 (Unwanted Beam Loss). Two invited plenary talks relevant to WG2 were presented in the plenary sessions and several WG2 poster presentations were provided in the poster session. All these presentation slides can be seen in [1].

In order to make a summary report for WG2, we classified WG2 topics and issues for small collaboration reports as follows:

- 1) Design principles learned from existing ERLs
- 2) Test ERL designs
- 3) Lightsource ERLs
- 4) ERLs for high energy and nuclear physics
- 5) Code survey for ERL simulation
 - a) Space Charge
 - b) IBS/Touschek scattering
 - c) CSR
 - d) Surface physics/secondary electron production

We assigned each of them to one or several authors and encouraged to finally produce a set of stand-alone papers for these topics and issues. Separately we asked all of them to produce a one- or few-page manuscript (with figures) for making a summary paper and could receive manuscripts from some of the authors. Here we will present a WG2 summary based on these manuscripts.

LESSONS FROM EXISTING ERLS

Accelerator Transport Lattice Design Issues for High Performance ERLs: S. Benson and D. Douglas (JLAB)

When designing an ERL there are some things that are good to remember:

1. ERLs are 6-dimensional systems. They are essentially time-of-flight spectrometers (well, maybe turned inside-out).
2. They are transport lines (not rings). The beam does not achieve equilibrium. The rms beam size σ is therefore not meaningful.
3. ERLs do not have closed orbits. The overall transport need not be betatron stable so there is no guarantee there are unique “matched” Twiss parameters. Therefore the actual beam envelope and the matched beam envelopes are not necessarily the same.
4. ERLs do not recover energy, they recover RF power – and power flow management is critical to their operation.

Design Process The design of an ERL should start with the user requirements, which flow down to the longitudinal match, which sets the RF drive requirements, and then the transverse match, which dominates acceptance. Chromatic/geometric aberration management is then carried out. Finally the collective effects and power flow are calculated, problems uncovered, and one iterates the process until one is satisfied.

Longitudinal Matching in an ERL Longitudinal matching requires the use of RF to compensate beam quality degradation and provide for energy compression during energy recovery. One must use the RF power to cover the user’s power draw. Note that the accelerated and decelerated beams may balance imperfectly during energy recovery. Because of this the beam dump energy is not necessarily the same as the injected energy.

The longitudinal scenario for the FEL at Jefferson Lab is as follows. Inject a long bunch to avoid space charge effects. Accelerate on the rising part of the RF waveform. Compress the bunch using both linear and non-linear momentum compactions ($M_{56}, T_{566}, W_{5666}$). One then uses the linear and non-linear compactions of the exhaust arc to match the bunch from the FEL, which is still short but now has a large energy spread, into the linac and compress the energy spread to the dump. Note that the deceleration phase depends only on the exhaust full energy spread. This is because the entire bunch must

precede the trough of RF waveform. This means that the two beams are not necessarily 180° out of phase and not all the power is recovered. This is called incomplete energy recovery. Required phase bite is $\cos^{-1}(1 - \Delta E_{\text{FEL}}/E_{\text{LINAC}})$. At modest energy this is >25° at RF fundamental for 10% and >30° for 15%. With this large a phase spread one generally needs correction to third order (octupoles).

The longitudinal transport to the wiggler is essentially a parallel to point image while the wiggler to dump is point to parallel. Because of this, the energy and energy spread at the dump do not depend on the laser exhaust energy spread or efficiency. Finally note that chicanes are not necessary for bunch compression and that harmonic RF is not necessary for linearization of the longitudinal phase space.

Operationally the longitudinal match relies on bunch length measurements at full compression using a Martin-Puplett Interferometer, and longitudinal transfer function measurements of R₅₅, T₅₅₅, and U₅₅₅. Such measurements are shown in Fig. 1 for a nominal bunch (red curve), for mis-matched R₅₆ (cyan and green curves), and for mismatched T₅₆₆ (purple and yellow curves).

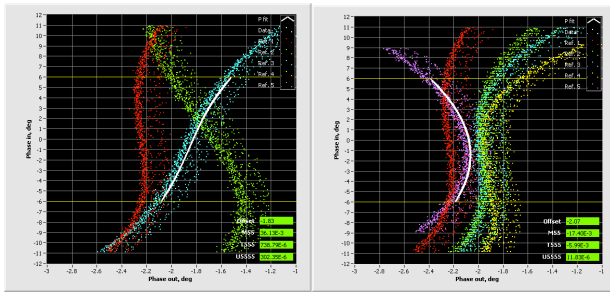


Figure 1: Phase transfer system measurements used to verify R₅₅, T₅₅₅, and U₅₅₅.

Transverse Matching Since the transverse match is the key driver of the acceptance, one must suppress chromatic/geometric aberrations.

One “old school” but very effective way to check the aberrations is to do momentum and aperture scans. One evaluates the spatial transfer function (4x4 matrix, $M(dp/p):(x_i, x'_i, y_i, y'_i) \rightarrow (x_f, x'_f, y_f, y'_f)$) and reference orbit $((0,0,0,0) \rightarrow (x_o(dp/p), x'_o(dp/p), y_o(dp/p), y'_o(dp/p)))$ at numerous momenta over some range.

One then uses the result to propagate notionally matched beam envelopes for monoenergetic beam for each momentum. One then designs the system to keep $\beta(dp/p)$, $\alpha(dp/p)$, $x(dp/p)$, $x'(dp/p)$,... invariant over the full momentum range. One typically has to invoke multiple sextupole families and/or construct destructive interferences amongst quad telescopes. One must avoid introducing *geometric aberrations* when correcting chromatics. Chromatic scans for the IR-Demo accelerator are shown in Fig. 2.

Experience from the ERLs at Jefferson Lab has shown that low loss energy recovery is possible when these techniques are followed and that deviation from this setup leads to an energy spread dependent loss at the low energy end of the recovery transport where the orbits are adiabatically undamped.

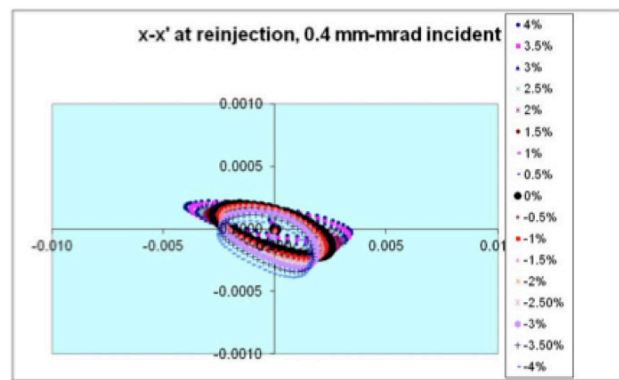
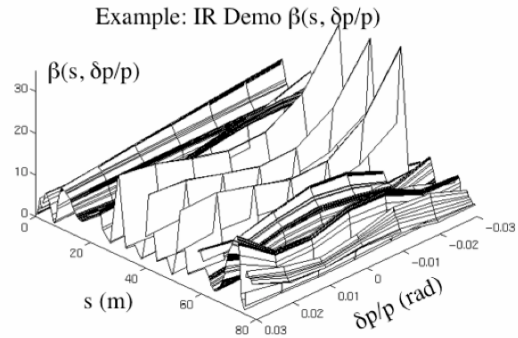


Figure 2: Momentum scans for the IR Demo FEL.

Collective Effects The whole reason to build an ERL is to generate high brightness, high power beams so collective effects are a logical consequence of that fact. Thus longitudinal space charge, coherent synchrotron radiation, resistive wall heating, and wakefields are always a problem. At higher currents, intrabeam scattering, Toushek effect, beam-gas scattering, and ion trapping will also be a problem. Halo is a major operational problem and has multiple sources, some of which might be the experiment itself (for example in nuclear and high energy physics applications). When designing an ERL one must provide locations to disentangle halo from core, large dynamic range diagnostics, and knobs for independent control of halo and core. For large systems one must also provide for collimation systems to protect long, small gap undulators. This must consist of multiple stages with appropriate phase separation.

Issues for Large Systems Large systems have to deal with multi-pass focusing & steering in linac. One must also make accommodations for beam dynamics (ISR, CSR, BBU, wakes, scattering, Halo). Another problem is the large dynamic range of the ERL, leading to the

potential for the longitudinal emittance exceeding the dump acceptance. A very important issue with large machines is magnetic field quality. This can provide significant obstacles to ERL performance. The basic idea is that differential field errors lead to differential angular kick which lead to differential betatron oscillations, which lead to accumulated path length error, leading to phase errors, leading to energy errors at the dump. This may have been source of performance-limiting loss in CEBAF-ER during operation with 20 MeV injection. When the full analysis is done one finds that the integrated magnetic field error tolerance is inversely proportional to the linac energy. One must provide a means to diagnose and correct the magnetic field errors.

Conclusions The path forward to higher power/higher energy/higher brightness is clear, but challenging.

Investigation of Beam Dynamics with Not-ideal Electron Beam on ALICE ERL: Y. Saveliev (Daresbury Laboratory)

ALICE is a multifunctional R&D facility at Daresbury Laboratory operating currently for ten projects in four different generic setups both in energy recovery and non-energy recovery modes. The range of parameters is wide: beam energy 12-28 MeV, bunch charge 20-100 pC, required energy spread from ~10 keV to 100 keV, and the bunch length from several ps down to sub picoseconds. Two major operating modes are for generation of infrared light with an IR FEL (tunable with 8 μ m nominal wavelength) and for broadband coherent THz radiation.

Depending on mode of operation, the first superconducting (SC) cavity of the booster (BC1) in the injector is set to off-crest phases of -10 to -20 deg. Generally, setting the BC1 phase farther off-crest improves the overall “quality” of the longitudinal phase-space in terms of combined uncorrelated energy spread and all imperfections of the phase space. The second cavity, BC2, compensates the energy chirp from BC1 and is set +10 to +40 deg off-crest. Note the phases quoted are in terms of the RF wave, not the bunch. The main linac cavities phases are chosen to (i) minimize energy spread if required; (ii) compensate a positive energy chirp from the injector and (iii) introduce a specific negative energy chirp for further bunch compression in the magnetic chicane. The linac off-crest phases are normally 0 to +16 deg.

Switching the machine from one mode of operation to another is often required on nearly daily basis. The adopted strategy for ALICE is that the beam energy in the injector is always kept constant of 6.5 MeV. Restoring of the setups relies on accurate, within a degree, phasing of all five RF cavities - the NC buncher pillbox cavity and the booster and the main linac each containing two SC cavities. The buncher zero-crossing is accomplished using the downstream BPM as a time-of-arrival monitor. The SC cavities are crested using downstream non-zero dispersion sections and predefined off-crest phases are set with calibrated phase shifters.

Beam dynamics investigation at nominal 60 pC bunch charges is hampered by irregular shape of beam images on screens where “two beams” can be often identified. This feature was recently investigated in more detail. Transversely, the two beams emerging from the booster are characterized by different size and divergence. Setting the second booster cavity at zero-cross phase allowed to imprint a specific energy chirp upon the electron bunch thus, in combination with the energy spectrometer, providing a means for evaluating the longitudinal structure. The two beams were found to be separated longitudinally. An example with the buncher power set deliberately high is shown in Fig. 3 and the longitudinal distance between the beams was measured to be 27 ps.

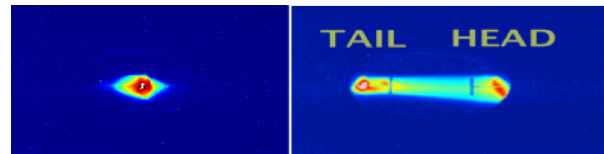


Figure 3: Two beams structure in non-zero dispersion section at high buncher power. Left – lower BC2 gradient just enough to equilibrate the energies of two beams. Right – at higher BC2 gradient to ensure energy separation between the two beams.

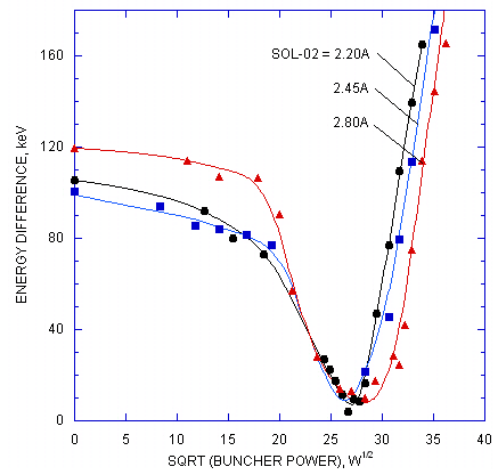


Figure 4: Energy difference between two beams in the injector as a function of buncher power at three different settings of the focusing solenoid. The energy chirp introduced by the second booster cavity BC2 is kept constant. Bunch charge is 60 pC.

The beams separation depends strongly on the buncher power (longitudinal compression) and on the strength of the solenoid located upstream of the booster (transverse focusing), see Fig. 4. This suggests that the space charge during the initial stage of the beam acceleration is an important factor in “two beams” formation and longitudinal separation between them. The other factor

could be temporally non-uniform laser pulse on the photocathode of the DC HV gun. ASTRA simulations suggest that the two beams could be formed with both, “flat” and “spiky”, laser pulses.

Currently, the formation of the two beams on ALICE could be amplified by low DC gun voltage of 230 kV and potentially non-uniform temporal laser pulse profile. Increasing the gun voltage should alleviate the problem but not eliminate it. The “two beams” could be therefore a feature of all injectors with DC photoelectron guns where acceleration in the first linac starts from non-relativistic electron energies (500 keV or lower).

Further experiments on ALICE will be conducted after installation of the large gun ceramic that will allow to increase the gun voltage to the design value of 350 kV. This will be complimented by measurements at various laser pulse profiles.

COMPACT ERL TEST FACILITIES FOR LIGHT SOURCES

Currently there are no less than four ERL test facilities being planned or under construction in order to gather experience with ERL technology and prepare for large multi-GeV ERL light sources. There are two Chinese

projects, one at the Peking University [2] and one at the Institute for High Energy Physics (IHEP) also in Beijing [3]. KEK at Tsukuba, Japan is currently setting up a compact ERL extendable to a two-loop configuration [4] and BERLinPro at the HZB in Berlin, Germany, has been funded in October 2010 [5].

The common understanding is, that the ERL based radiation sources promise extremely attractive features, but that the technologies involved are so challenging, that they should be investigated and prepared in a test facility, which also covers the need for personal training. Common goals to all test facilities are to:

- Demonstrate high charge, low emittance bunches from the gun
- Gather experience with 1.3GHz superconducting accelerating structures
- Produce high average current, high brightness electron beams
- Demonstrate energy recovery
- Investigate high current effects like BBU, CSR, halo formation, space charge etc.

Table 1: Listing of Main Parameters of Four Compact ERL Projects

	units	Peking University	IHEP Beijing	KEK	BERLinPro
Gun		DC-SRF	DC 500KeV	DC 500keV	SRF
Bunch charge	pC	60	77	7.7-77	77
Current	mA	1.56	10	10-100	<100
Booster				3x2-cell	3x2cell
Merger		Dogleg 20° – sector dipoles	Chicane – 6 quads	Dogleg 16°– 2 quads	To be decided
Injection energy	MeV	6	5	5-10	5-10
Linac		1.3GHz 2x9cell TESLA	1.3GHz 2x7cell	1.3GHz (2-8)x9cell TESLA	1.3GHz 3x7cell
Energy	MeV	30	35	35-125/245	50
Emittance	mm mrad	4	2	0.01-1	<1
Energy spread	%	0.3	0.5	0.01-0.02	
Bunch length (rms) / compressed	ps	4 FWHM	2-4 / 0.2-0.5	1-3 / 0.1	2
R56 / T566		0.525/42.8	0.16-0.19	0.1 – 0.15	-0.4-0.4
Arc bends		4x45°	45°-90°-45°	4x45°	4x45°
Arc quads		5	3 x 2	3 x 2	7
Sextupoles		2	Under consideration	2 x 2	2
Insertion device	No of poles*period length[cm]	40*3	25*6	Laser Compton THz	Not in first stage

In Table 1, the main design parameters for the four projects are listed. The largest deviation between the projects can be found in the gun. While KEK and IHEP employ DC guns, Peking University puts much effort in developing a novel DC-SRF gun, and the HZB has set up a gun laboratory to develop an SRF gun. All guns, though, are expected to deliver the same 60-77 pC, 2-3 ps low emittance bunch, which is then accelerated to 5-10 MeV before it is injected into the recirculator. KEK and Peking University use a dogleg merger with quadrupoles and sector magnets respectively for dispersion

suppression. IHEP may proposes two different 3-4 dipole chicanes with two different injectors aiming at studying the possibility of accelerating the two beams from two gun simultaneously in the same main linac, one is directly for FEL experiment and another for ERL. However in the first phase of IHEP, only one DC-gun injector will be considered. The merger decision for BERLinPro is still open. The superconducting main linacs all run at 1.3 GHz, TESLA technology has been adopted in Peking University and an original 9-cell cavity with enlarged beam pipes and on-axis HOM absorbers has been

developed at KEK. The other projects focus on 7 cell structures. All recirculating arcs start with 45° dipoles to keep the dispersion low. While IHEP uses a 90° magnet at the center, KEK split this magnet into two 45° magnets. To control the path length up to half the RF wavelength the four 45° magnets are movable along the orbit for the upgrade to the two-loop configuration. BERLinPro and Peking University introduce one and three quadrupoles, respectively, between the two inner dipoles, providing more flexibility to fit R_{56} and the Twiss parameters simultaneously. Only the two Beijing projects include considerations for undulators/FEL operation from the beginning, while KEK has plans for laser-Compton scattering (LCS) x-rays and THz radiation without an undulator at the compact ERL.

Only a few contributions concerning nonlinear effects were made during this session. IHEP and BERLinPro comment on shaping the beta functions in the linac in order to suppress CSR and BBU, while BERLinPro sees matching difficulties between the second arc and the linac due to BBU conditions. KEK tries to minimize CSR effects by minimizing the betatron functions in the arc; IHEP uses Twiss parameter (α_x) matching in front of the first arc. Peking University and IHEP apply an energy spread suppression technique in the second arc to compensate the increase in energy spread due to the insertion devices.

ERL Test Facility at Peking University: S. Huang (PKU)

In slight deviation from the above mentioned goals, the focus of the ERL Test Facility at Peking University is to build an ERL-based radiation source (including an FEL) and especially to develop the superconducting photo-injector.

At present, the DC-SRF photo-injector and 2K cryogenic system have been installed. Preliminary beam loading tests on the injector agree well with dynamics studies and indicate that it is expected to produce electron beams with bunch charge of 60 pC, repetition rate of 26 MHz and normalized emittance better than 4 mm-mrad. The optics design for the ERL test facility has been carried out according to these characteristics.

The building to host the facility and the layout of the LHe transfer pipes pose constraints to the optics of the ERL test facility. The distance between the south straight section and north straight section is 4 m and the east arc is very close to the shielding wall, which leads to very compact arcs. However, as a test facility, the optics design gives as much flexibility for ERL and ERL-based FEL experiments as possible. For cost reason, the beta functions of the facility are controlled within 16 m, and the dispersion is within 1 m. Shown in Fig. 5 are the overall lattice, beta functions and dispersion.

Beam dynamics studies are ongoing. Further optimization of operation parameters for DC-SRF injector will be performed to improve the characteristics of the electron beam, especially to lower the transverse and longitudinal emittance.

ISBN 978-3-95450-145-8

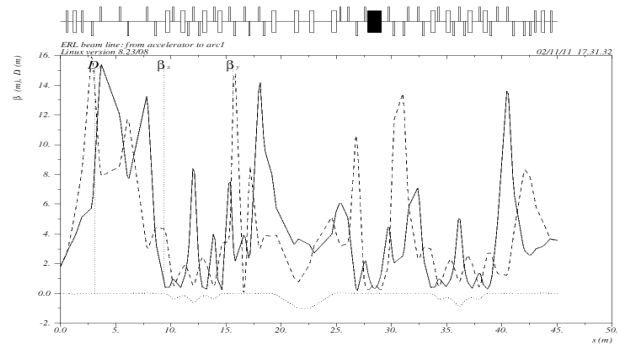


Figure 5: Beta functions and dispersion for the Peking University ERL test facility.

ERL Test Facility at IHEP: J. Wang (IHEP)

The layout of the 35 MeV, 10 mA ERL test facility at IHEP is as shown in Fig. 6. A 500 kV DC-gun and 5 MeV injector will provide the low emittance beam for the main linac. Two TBA arcs (each consist of 45° - 90° - 45° bending magnets, with some quads and sextupoles) and two long straight lines for the main linac and for the insertion device, respectively. The 77pC, 2ps bunch is compressed to 0.25-0.5ps with the 1st TBA arc to achieve high CSR-THz and/or THz-oscillator powers produced in a followed undulator. The emittance growth due to CSR during the bunch compression can be minimized to about 30% by employing envelope matching methods. The BBU threshold current could be higher than 260 mA by a code simulation. The energy spread minimization down to 1.5% of the decelerating beam is preliminarily studied by choosing the linac RF phase and R_{56} of the 2nd TBA arc. The 77pC, 5MeV, 2pS beam injection into the main linac is also preliminarily simulated with some beam emittance and bunch length growth mainly due to the space charge effect. Further studies are underway.

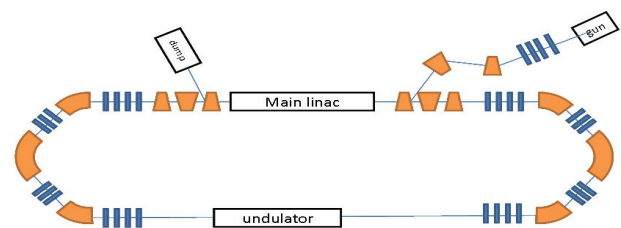


Figure 6: The layout of test ERL at IHEP, Beijing.

Compact ERL Test Facility at KEK: M. Shimada (KEK)

Also at KEK the long-term plan is to replace the photon factory by a combined ERL-XFEL-O facility. In a two stage approach, a 3 GeV ERL will be set up, which in a later stage and an electron beam accelerated twice to feed a 6-7 GeV XFEL-O without energy recovery. As a test

facility, the compact ERL extendable to 2-loop configuration is under construction in KEK site. For the first commissioning in 2013, one cryomodule including two 9-cell superconducting cavities will be installed in the one loop ERL. The full energy is 35 MeV. The compact ERL will be gradually upgraded to double loop scheme and the full energy of 245 - 250 MeV (injection energy is 5 - 10 MeV). The layout of the double loop is shown in Fig. 7.

Start-to-end (S2E) simulation is started to evaluate the beam quality and the emittance growth due to the space charge effect and CSR wake. Space charge effects, which are significant at low electron energy, are simulated by the code, General Particle Tracer (GPT). It is only used for injector and dump beam at less than 65 MeV because it consumes too much CPU time. The 6D electron distribution in the double loops is simulated by particle tracking code 'elegant' including the CSR wake.

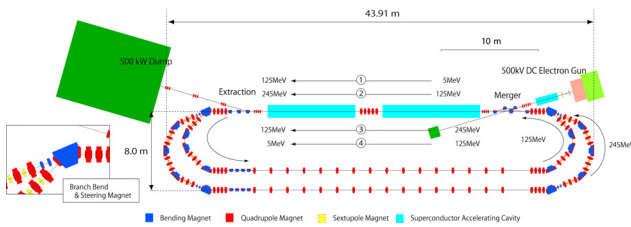


Figure 7: Layout of double loop compact ERL at KEK.

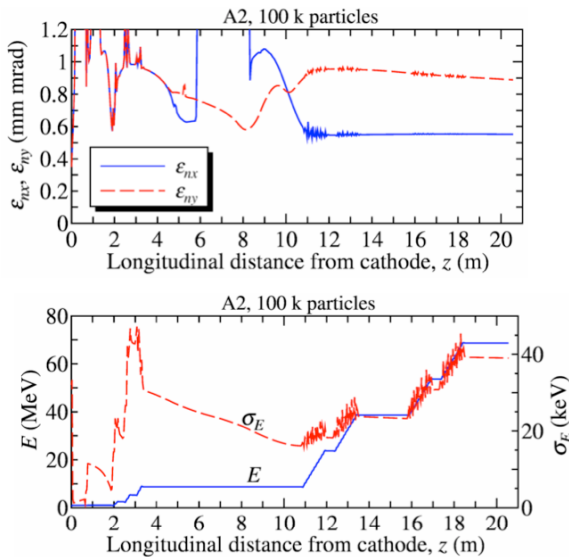


Figure 8: Optimization results of injector: transverse normalized emittance (upper) and electron energy and energy spread (lower).

Figure 8 shows simulation results of injector. The injection energy is 8.7 MeV and the electron charge is 77 pC. The normalized transverse emittance at 65 MeV is 0.54 mm-mrad[H] and 0.89 mm-mrad[V], which are restricted by the optical matching with the double loops shown in Fig. 9. The optical functions of double loops are

designed using dummy loops, which are composed of quads and drifts. The horizontal emittance increases at each arc in the double loops due to the CSR wake. It results in 5mm-mrad at the straight section in the outer loop. Further optics optimization will be done to reduce the horizontal emittance.

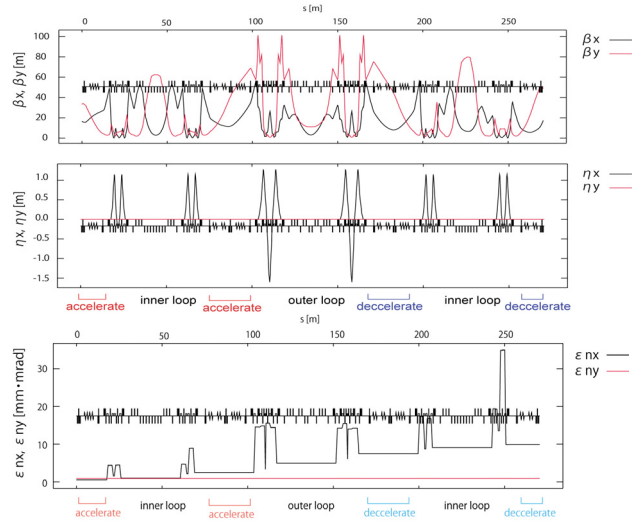


Figure 9: Betatron function (upper), dispersion function (middle) and transverse emittance of double loop compact ERL.

BERLinPro – ERL Project in Berlin, Germany: B. Kuske (HZB)

BERLinPro, a high current, low emittance ERL test facility at the HZB has been funded in October 2010. Due to the restricted financial frame, the project goals had to be de-scoped mainly by cutting down on the SRF systems. The layout of BERLinPro is shown in Fig. 10. The energy has been lowered to 50 MeV, which results in a severe cut in the radiation shielding requirements. The pulse-shaping unit for the cathode laser has been canceled. Figure 11 shows the effects of the pulse shaping on the bunch current profile and Figure 12 shows the bunch length dependence on laser pulse and bunch length development between the cathode and booster. The layout of BERLinPro could be adapted to the new requirements without severe performance degradation.

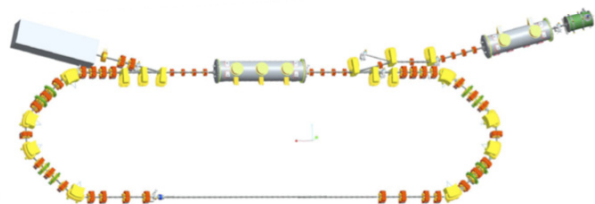


Figure 10: Layout of BERLinPro.

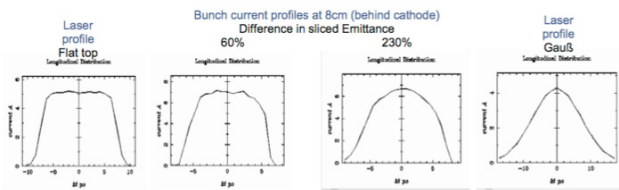


Figure 11: Laser pulse shape and current profile of the bunch behind the gun cavity for a flat top laser pulse (left) and a Gaussian laser pulse (right). The minor differences are further washed out and are negligible behind the booster longitudinally as well as in the transverse phase space.

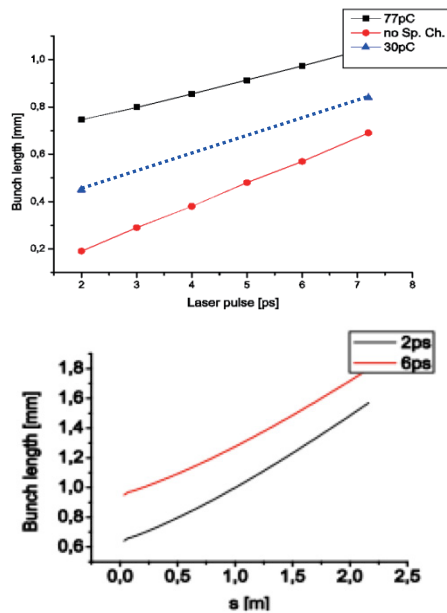


Figure 12: Upper: Bunch length as a function of the laser pulse length, behind the gun cavity for 77 pC (black) and without space charge (red); without space charge, velocity bunching shrinks the bunch to ~1/3 of the laser pulse length. Space charge counteracts this process. Lower: Bunch length development between cathode and booster for a 2 ps and a 6 ps long laser pulse. The difference in bunch length is only ~15%.

Beam dynamics studies for an injector with a half-cell SRF gun have been performed for low gun phases (10° off zero phasing) and show that longitudinal bunch properties are dominated by velocity bunching and space charge rather than by the initial longitudinal laser profile or its length.

The reduction from 5 to 3 cavities in the booster module increases the RF focusing, as the injection energy remains at 5-10 MeV. The increased focusing can be compensated by a different solenoid setting. The first cavity can be used for velocity compression of the bunch. The two later cavities will have enough transmitter power for acceleration. The emittance behind the booster is 0.87 mm mrad for a 6 ps bunch.

ISBN 978-3-95450-145-8

It has been shown that for the 4 dipole chicane merger the number of quadrupoles necessary to keep the emittance below 1mm mrad grows with the shortening of the bunches, as space charge increases.

The BBU instability can be controlled by matching the beta functions in the linac. BBU conditions result in a minimum in both beta functions in front of the linac. To match these conditions, it seems helpful to keep the distance between the end of the second arc and the linac as short as possible and to provide high matching flexibility in the arc. For this reason an extra quadrupole has been introduced between the central 45° dipoles in the arc, and a scheme to include the last arc dipole into the chicane for the high energy beam is considered.

LIGHTSOURCE ERLS

3-GeV ERL at KEK: N. Nakamura(KEK)

KEK has a future project to construct an ERL-based light source as the successor of two existing SR sources at the Photon Factory, 2.5-GeV PF ring and 6.5-GeV PF-AR [6]. In the first stage of this project, a 3GeV ERL will be constructed with many insertion devices providing super-brilliant and/or ultra-short SR in the VUV to hard X-ray region. In the second stage, a 6-7 GeV XFEL-O, which can generate fully coherent X-rays, will be constructed. The schematic view of the ERL-based light source is shown in Fig. 13. In the XFEL-O operation, an electron beam is accelerated twice by the main linac without energy recovery and fed to the XFEL-O. The design study of the 3-GeV ERL was recently started. A test ERL, the compact ERL(cERL), is under construction in the KEK Tsukuba Campus and will be commissioned in 2013 to demonstrate excellent ERL performance toward the ERL-based light source project.

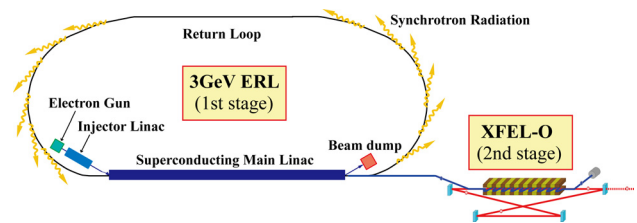


Figure 13: Schematic view of the ERL-based light source project at KEK.

Injector design and optimization of an ERL are very important for transporting high-current and low-emittance beams to the main linac without serious degradation of beam quality. The injector of the 3-GeV ERL will be designed based on design and operational experiences of the cERL injector. The cERL injector consists of a 500 kV photo cathode DC gun, two solenoid magnets, a buncher cavity, three superconducting RF cavities, five quadrupole magnets, and a merger consisting of three rectangular magnets with the bending angles of -16, 16 and -16 degrees, and two quadrupole magnets. By multi-

objective optimization with a genetic algorithm, the horizontal and vertical normalized emittances at the exit of the cERL injector were successfully optimized to be smaller than 0.6 mm mrad for the bunch length of 0.6 mm (2 ps), the beam energy of about 8.5 MeV and the bunch charge of 80 pC (more than 100 mA at 1.3 GHz repetition). In the injector of the 3-GeV ERL, the emittance should be reduced further to improve the light source performance. Higher injector energy and higher gun voltage are possible approaches, in addition to improving the injector design.

The main linac will consist of more than 200 superconducting (SC) 9-cell cavities, each of which has a moderate accelerating field of less than 15 MV/m to suppress field emission causing beam halo and radiation hazards. Quadrupole triplets are placed at every eight SC cavities for focusing. The optics of the main linac is mirror-symmetric for acceleration and deceleration and designed so that the betatron function is well suppressed for achieving a high BBU threshold current.

The return loop of the 3-GeV ERL have 28 TBA cells with 22 x 6 m and 6 x 30 m long straight sections for insertion devices. The bending radii of the bending magnets are sufficiently long to suppress emittance growth and increase of energy spread due to the incoherent synchrotron radiation (ISR) effects. Each of these cells is achromatic and isochronous and has a horizontal betatron phase advance of π per two cells so that CSR kicks to the beam can be considerably cancelled. Figure 14 shows preliminary optical functions of the main linac and the return loop. A bunch compression scheme should be studied by using off-crest acceleration in the main linac and non-zero R_{56} in the return loop in order to generate ultra-short bunches less than 100 fs. A chicane system changing a path length by a half RF wavelength is also needed for switching from energy recovery operation to XFEL-O operation. The tentative layout of the 3-GeV ERL with the XFEL-O in the KEK Tsukuba Campus is shown in Fig. 15.

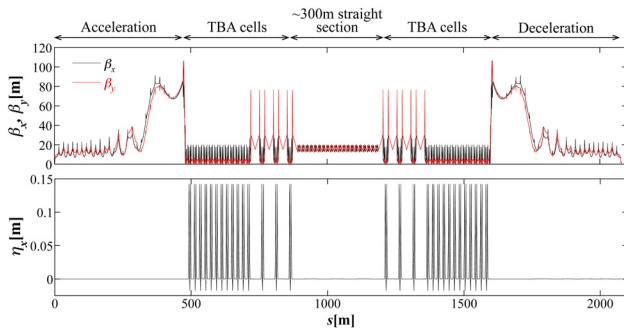


Figure 14: Betatron function (upper), dispersion function (bottom) of the main linac and the return loop of the 3-GeV ERL.

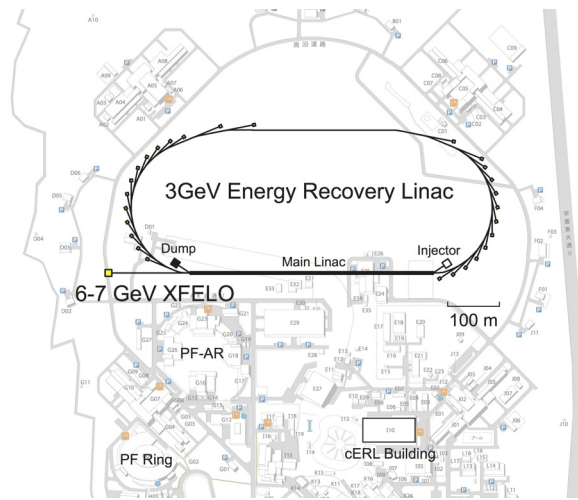


Figure 15: Tentative layout of the ERL-based light source in the KEK Tsukuba Campus.

Cornell ERL: C. Mayes (Cornell U.)

The Cornell Laboratory for Accelerator-based Sciences and Education (CLASSE) is planning to build a hard x-ray ERL-based lightsource operating at 5 GeV at 1.3 GHz. The Cornell ERL will nominally provide three operating modes: High Flux operating at 100 mA, 0.3 mm-mrad normalized emittance and 2 ps bunch duration, High Coherence operating a reduced current of 25 mA with an enhanced normalized emittance of 0.08 mm-mrad, and Short Bunch operating at reduced current and short bunches of 100 fs duration.

This project is extensively documented in the Cornell ERL Project Definition Design Report (PDDR) [7], which begins with a chapter on the history and motivation for an ERL at Cornell. The accelerator chapter comprises the bulk of the PDDR, and includes sections on accelerator physics, the vacuum system, the injector, the linac, the RF systems, the electron transport lines, the beam stops, startup procedures, beam diagnostics and control, control system integration, and machine protection. A separate chapter outlines novel x-ray experiments and beamlines that are well-suited for ERL-quality beams. In addition to a chapter on conventional facilities, this document is supported by an economic impact report, a draft environmental impact report, a design for a new x-ray science building, a tunnel design and review, a proposal for the construction of the electron beamlines, and two proposals for the cryogenic system.

In preparation for this facility, CLASSE continues to perform essential research and development of key ERL technologies, and currently operates a prototype ERL injector, a dedicated photocathode laboratory, and an SRF laboratory. Novel insertion devices such as the ‘delta’ undulator are also being developed. Some recent achievements, including new world-record currents from the injector, are described in [8].

Multi-turn ERL X-Ray Source (MARS):

G. Kulipanov (BINP)

A conception of the multi-turn accelerator-recirculator source (MARS) was proposed for realization of a fully spatially coherent X-ray source in 1997 [9]. The Novosibirsk ERL with two orbits and two FELs is operated towards MARS [10]. In order to generate fully spatially coherent undulator radiation with wavelength $\lambda = 0.1\text{nm}$, emittance of electron beam should be decreased to diffraction limit $\varepsilon_{x,z} < \lambda/4\pi \approx 10^{-11}\text{m}$ at $E = 5\text{-}6\text{ GeV}$. Since high current up to 100 mA does not increase and even decreases the brightness sometimes, the average current does not need to be more than 10 mA. Radiation should be used only from three types of undulators with number of periods $N_{u1}=100$, $N_{u2}=1000$, $N_{u3}=10000$, not from bending magnets to keep the photon flux at the level of the 3rd generation sources.

The main disadvantage of the multi-turn ERL scheme with one accelerating structure is that two electron bunches (accelerating and decelerating) are circulated simultaneously at almost all the magnetic arcs. Radiation at an undulator in such an arc is generated by both accelerating and decelerating beams. This requires precise alignment and complicated control of the electron beams. Therefore, as shown in Fig. 16, it has been proposed to use scheme with two accelerating sections and separated magnetic arcs for accelerating and decelerating beams [10].

In this scheme, cascade injection system, which consists of two preliminary acceleration sections, is employed. This injection system accelerates electrons to energies 50 MeV and 400 MeV. This relatively high injection energy simplifies focusing of electron beams with different energies traveling simultaneously in the accelerating structure. Moreover, it increases the threshold current of the transverse beam breakup (BBU). For the same reasons, two asymmetrical main accelerating structures (0.7 and 1.9 GeV) are used. Use of the cascade injection and energy recovery decreases radiation hazard and the induced radioactivity due to the low energy of electrons at the dump (5-8 MeV), and leads to reduction in the cost of building and RF power supply for the injector.

Another advantage of the split accelerating structure is a possibility of servicing the multi-user community. A scheme with one undulator in Fig. 16 can be extended by installations of the long undulators into bending arcs 4. There are 7 undulators for 5.6 GeV, and 4 undulators for 3.7 GeV, 3 GeV and 1.1 GeV. To simplify the radiation output the magnetic arcs are separated both horizontally and vertically. A schematic view of MARS with these features is shown in Fig. 17.

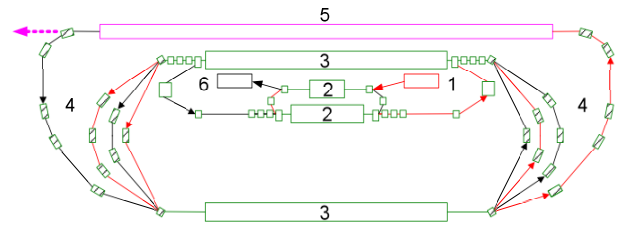


Figure 16: The simplest scheme of accelerator with 2 separated accelerating structures: 1-injector, 2 –two preliminary accelerating structures, 3 – two separated linacs, 4 – magnetic arcs, 5 – undulator, 6 – dump.

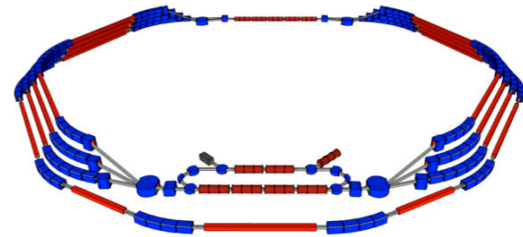


Figure 17: Scheme of MARS with main features: cascade injection, two accelerating structures, separated bending arcs, vertical separation of radiation beamlines.

Table 2: Parameters of MARS

Energy	5.6 GeV
Average current	10 mA
Peak current	10 A
Normalized emittance	0.1 mm mrad
Relative energy spread	$2.2 \cdot 10^{-5}$
SR sources	19 Undulators ($N_u \sim 10^2$, $N_u \sim 10^3$, $N_u \sim 10^4$)
Geometrical sizes	1x1 km

Since the magnetic structure of this accelerator is not an isochronous, all three types of beam-cavity interaction instabilities are excited (beam-loading, HOM transverse and longitudinal BBU). In the simplest case of single-cavity model, threshold current of transverse BBU was estimated and found that the threshold current of more than 10 mA can be achievable [11]. For beam-loading instability, simulations showed that there are areas of the stable accelerating phases. The main parameters of MARS are listed in Table 2.

Laser Compton Scattered Gamma-ray Sources:
R. Hajima(JAEA)

The combination of an ERL and a high-power mode-locked laser realizes significant improvement of γ -ray sources based on laser Compton scattering (LCS) [12]. In order to obtain a high-flux γ -ray, it is necessary to increase the density of both electrons and photons at the collision point. An electron beam of small emittance and high-average current is essential to high-flux γ -ray generation via Compton scattering. The combination of an ERL and a laser enhancement cavity is, thus, a promising source of high-flux γ -rays. Figure 18 shows a schematic view of an ERL γ -ray source. At the collision point, electron bunches circulating the ERL loop collide with laser pulses stored in an enhancement cavity, which is a high-finesse Fabry-Perot optical resonator to stack a train of laser pulses from a mode-locked laser.

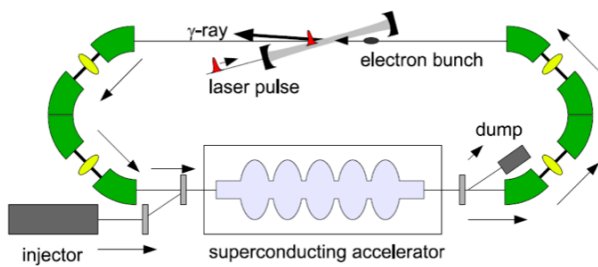


Figure 18: A schematic view of LCS γ -ray source based on an ERL and a laser enhancement cavity.

The effect of electron beam emittance on the broadening of γ -ray bandwidth becomes as small as the effect of laser diffraction when the normalized emittance ϵ_n is equal to $\lambda/4\pi$ (λ : laser wavelength). For a typical laser wavelength, $1\mu\text{m}$, the normalized emittance is 0.08 mm-mrad , which is a similar value to the required emittance for ERL-based synchrotron radiation sources to obtain coherent hard X-rays.

Figure 19 shows the γ -ray spectrum calculated for a 2-MeV γ -ray source using a 350-MeV ERL in the narrow-bandwidth mode (10 pC, 0.1 mm-mrad, 130 MHz). For a 0.05-mrad aperture, the γ -ray bandwidth is 0.2% (FWHM). In the limit of small aperture at the narrow-bandwidth mode, the γ -ray bandwidth is restricted by the electron beam energy spread. Possible use of low-frequency spoke cavities achieves further reduction of LCS γ -ray bandwidth because of the smaller RF-correlated energy spread of electron beams. It should be noted that a LCS γ -ray source based on a storage ring has a limitation of γ -ray bandwidth resulting from a large energy spread of electrons at the equilibrium state, where the quantum excitation is balanced with the longitudinal damping.

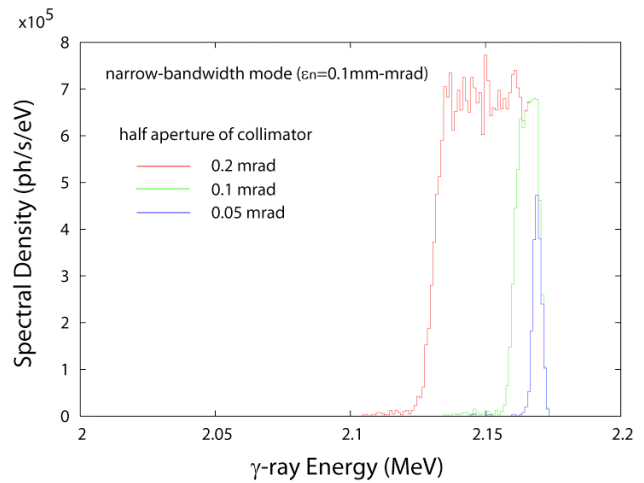


Figure 19: Calculated γ -ray spectrum from a 2-MeV γ -ray source using a 350-MeV ERL in the narrow-bandwidth mode (10 pC, 0.1 mm-mrad, 130 MHz) with various sizes of on-axis collimators. Collimator half aperture is 0.2 mrad, 0.1 mrad and 0.05 mrad.

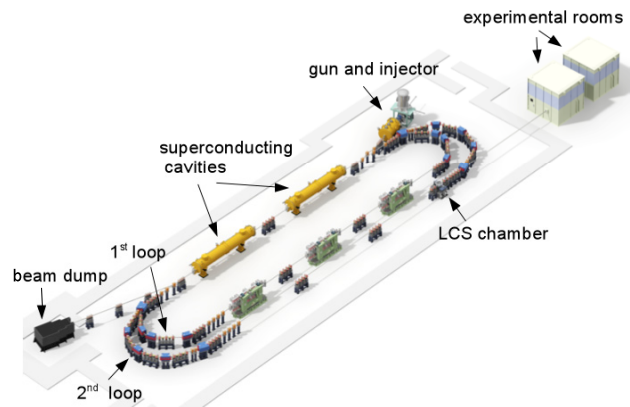


Figure 20: A schematic view of the LCS γ -ray experiment at the Compact ERL of KEK.

In order to demonstrate the performance of ERL γ -ray source and explore applications of ERL γ -ray sources to nuclear security and safeguards purposes, JAEA has launched a 3-year program (2011-2013) supported by Ministry of Education, Culture, Sports, Science and Technology (MEXT) in Japan. The program aims at generation of a high-flux and narrow-bandwidth γ -ray beam at the Compact ERL in collaboration with KEK. Application of the γ -ray to non-destructive measurement of isotopes is also planned. Figure 20 shows a schematic view of the proposed experiment at the Compact ERL.

CODE SURVEY FOR ERL SIMULATION

Survey on CSR codes - Contributors: G. Bassi, W. M. Fawley, R. Li, A. Novokhatski, K. Oide, J. Qiang, B. Terzic, J.-L. Vay, and D. Zhou

The paper published by G. Bassi, et al. [13] gave a comprehensive overview of the CSR codes developed before 2006. Since then, tremendous efforts have been expended in developing new codes as well as investigating new numerical techniques. The present survey focuses on progresses of code developments since ERL2005. The purpose is to highlight the progresses of CSR code developments as well as new numerical techniques in the past several years. The new CSR codes are classified into 1D approach, Newton-Maxwell approach, approach with paraxial approximation, Vlasov-Maxwell approach, and Particle-In-Cell (PIC) approach. This classification is based on the numerical methods adopted by the CSR codes [14]. Another scheme is to classify the CSR codes into 1D, 2D, or 3D based on the simulated dimensions in real space.

1D approach CSR is included in the parallel beam dynamics code IMPACT [15]. In the code, the CSR model is a combination of the longitudinal CSR wake function to account for radiation fields and the three-dimensional short-range space charge fields [16]. The longitudinal wake function follows a physical model developed by Saldin et al. [17] and simplified by Borland [18] and by Stupakov et al. [19] under relativistic approximation. The line density function λ is obtained using a linear macroparticle deposition. This function and its derivatives are smoothed using a first-order Savitzky-Golay filter [20] or a custom designed local filter [21]. The CSR wake field is calculated following a direct double summation. The three-dimensional space-charge fields are calculated inside a locally rotated beam framework along the bending trajectory using the Green function method. The convolution is done numerically on a three-dimensional mesh using an FFT based method [22].

Newton-Maxwell approach Novokhatski developed a new 3D approach [23] to study CSR field dynamics. It is based on solving Maxwell's and Newton's equations. For this reason it can give fruitful information about the beam and field dynamics. It describes the radiation of a bunch in a metal chamber and includes geometrical wake fields. Another effect, especially important for the bunch compressors, is the acceleration or deceleration of a bunch due to the change of its shape and its position in a chamber. This method already predicted many new effects. The most important is the coherent energy spread. The numerical schemes are discussed in details in Refs. [24, 25]. The comparison with the THz measurements at ANKA is on the way.

Approach with paraxial approximation Since the mesh method by paraxial approximation was devised by Agoh and Yokoya [26], it has been extended by several

authors [27, 28, 29, 30] to calculate the CSR impedance in a single bending magnet or a series of bending magnets. By paraxial approximation, Maxwell's equations for CSR fields are simplified into a parabolic wave equations for the transverse electric fields.

Gillingham and Antonsen solved the parabolic equation in the time domain [27]. The space-charge effect was taken into account by keeping the dominant term of $1/\gamma^2$ in the field equation. In their code, an unconditionally stable integration method with transparent boundary conditions was implemented. It allows the use of a minimally sized computational domain about the bunch. The causality condition was explicitly enforced so that no portion of the fields can propagate faster than the speed of light. Stupakov and Kotelnikov solved the parabolic equation in the frequency domain [28] using mode expansion method. The beam is assumed to be ultrarelativistic. In a vacuum chamber with uniform cross section, the electromagnetic fields generated by a bunched beam can be decomposed over the eigenmodes of the chamber. A computer code based on using the Mathematica programming environment [31] was developed to calculate the CSR impedance for a toroid of rectangular cross section. The mode expansion method is quite general and, in principle, is applicable to arbitrary cross section of the toroidal pipe.

Oide developed a new code independently [29]. The code is basically a Helmholtz solver using a finite difference method. It accepts arbitrary shapes of the beam pipe. The most important nature is that the coupling between E_x and E_y at the boundary is introduced via an expression of the Laplacian at the boundary. It is done by numerical fudge factors which are determined through comparison between numerical and analytic solutions for solvable cross sections, square and round pipes. Another characteristic of the code is that it is embedded in the SAD code [32] to utilize the object-oriented script language of SAD and incorporation with other accelerator calculations as well as graphics interfaces, etc. A new code CSRZ was developed by Zhou [30] to investigate the longitudinal coherent synchrotron radiation (CSR) impedance for a single or a series of bending magnets. To calculate CSR impedance, the mesh method developed by T. Agoh and K. Yokoya [26] was adapted to the case of a curved rectangular chamber with variable bending radius. In the code, the curvature of the beam trajectory can be set to be an arbitrary function of the distance along the beam orbit. Thus it allows calculating CSR impedance generated by a single bending magnet, a series of bending magnets interleaved with drift chambers, or a wiggler.

Vlasov-Maxwell approach Vlasov-Maxwell solvers aim to study the electrodynamics evolution of the system self-consistently with a mean field theory approximation, i.e. the system is evolved under the influence of its own electromagnetic fields generated by the macroscopic, or mean, charge/current densities. With this approximation, microscopic or collisional effects are neglected. Bassi et al. developed a self-consistent 4D Vlasov-Maxwell

Monte Carlo code VM3@A (Vlasov-Maxwell Monte-carlo Method @ Albuquerque). Because the source comes from the Vlasov equation the (Maxwell) self-field is a mean field. Significant progress has been made since the previous overview on CSR codes [23]. A parallel self-consistent algorithm has been developed and applied to study CSR effects and the microbunching instability in bunch compressors [33, 34, 35, 36, 37].

PIC approach Terzic and Li developed a new 2D code for self-consistent simulations of coherent synchrotron radiation (CSR) in beams [38]. The new code is based on the 2D CSR code developed by Li [39, 40] but is of the particle-in-cell (PIC) variety: the beam bunch is sampled by point-particles, which are deposited on the grid. The corresponding forces on the grid are then computed using retarded potentials according to causality, and interpolated so as to advance the point-particles in time. The retarded potentials are evaluated by integrating over the path history of the bunch, with the charge and current densities at the retarded time obtained from interpolation of the particle distributions recorded at discrete time steps. Vay and Fawley proposed a numerical scheme to speed up the CSR calculation. It is based on a suitable choice of the proper Lorentz boosted frame [41]. Orders-of-magnitude improvement on CPU-time has already been demonstrated for simulations from first principles of laser-plasma accelerators [42], free electron lasers [43], and particle beams interacting with electron clouds [44]. In [45], it is shown that this approach can be utilized in CSR calculations to remove the imbalance between the different scales in space and time of the problem by performing the calculation in a suitable Lorentz-boosted frame. Unlike some other lab-frame based approaches [26] no approximation of the Maxwell equations is required. The boosted-frame scheme is implemented in the parallel PIC code Warp [46]. Their results to date suggest that fully electromagnetic and accurate simulation of beam compressors is possible in regimes of great interest for design of linac-based short wavelength free electron lasers.

CONCLUSIONS

Lessons from two existing ERLs, the JLAB ERL and ALICE at Daresbury Laboratory, are very instructive and we should learn design principles and operational experiences from the existing ERLs including the Novosibirsk ERL at BINP, the first multi-turn ERL in the world, which was presented in the WG2 session.

There are four test ERL projects for light sources being planned or under construction at Peking U., IHEP, KEK and HZB. Various parameters related to beam dynamics are listed for comparison of these ERLs and optics design and/or beam dynamics studies of each test ERL are also shown here. It is noted that a high-current test ERL for high-energy and nuclear physics is under construction at BNL. It may be effective for these facilities to share experiences of optics design and beam simulation,

because their accelerator energies, structures and scales are very similar.

Unlike the test ERLs, light-source ERLs have variety in their features. While the 3-GeV KEK ERL is a single-turn ERL with one accelerating structure and a 6-7 GeV XFEL-O, the 5-GeV Cornell ERL includes the existing ring CESR and two main accelerator sections. MARS project at BINP is a multi-turn 5-6 GeV ERL with split accelerating structure, a cascade injection system and separated magnetic arcs for accelerating and decelerating beams. Although these multi-GeV ERLs have many common beam dynamic issues for generating high brightness SR, they also have to solve issues peculiar to their projects. Gamma-ray ERL sources based on laser Compton scattering (LCS) are rather similar to test ERLs in many features and can share major beam dynamics issues with them. ERL projects for high energy and nuclear physics such as MESA, eRHIC and LHeC were also hot topics in this workshop and their beam dynamics issues should have been compared to one another and those of the other ERLs, though they are not described here.

Several simulation codes on CSR, space charge, IBS/Touschek scattering and field emission in a cavity and their simulation results were reviewed or presented in the plenary and WG2 sessions. CSR codes are systematically surveyed in this paper.

ACKNOWLEDGMENTS

We would like to thank the ERL2011 committees, all the contributors to the presentations and discussions in Working Group 2, and those who provide material for this paper.

REFERENCES

- [1] <http://erl2011.kek.jp>
- [2] S. L. Huang et al., "Optics Layout for the ERL Test Facility at Peking University", these proceeding.
- [3] S. H. Wang et al., "Design Studies on the ERL Test Facility at IHEP-Beijing", these proceedings.
- [4] M. Shimada et al., Proc. of IPAC11, San Sebastian, pp.1909-1911.
- [5] A. N. Matveenko et al., Proc. of IPAC11, San Sebastian, pp.1500-1502.
- [6] Energy Recovery Linac Preliminary Design Report (2012); N. Nakamura, Proc. of IPAC12, New Orleans, pp.1040-1044.
- [7] Cornell Energy Recovery Linac Project Definition Design Report, G. Hoffstaetter, S. Gruner, M. Tigner, eds. <http://erl.chess.cornell.edu/PDDR/> (2012).
- [8] C. Mayes *et al.*, Status of the Cornell ERL, ICFA Beam Dynamics Newsletter 58, pp. 112-118 (2012).
- [9] G. N. Kulipanov, A. N. Skrinsky, N. A. Vinokurov, J. of Synch. Rad. **5** (1998) 176.
- [10] N. A. Vinokurov et al., Proc. of IPAC10, Kyoto, pp.2427-2429.

- [11] G. N. Kulipanov et al., "Multi-turn ERL X-ray Source (MARS) Feasibility Study", these proceedings.
- [12] R. Hajima, "Laser Compton Scattered Gamma-ray Sources", these proceedings.
- [13] G. Bassi, et al., Nucl. Instrum. Methods Phys. Res., Sect. A 557, 189 (2006).
- [14] M. Dohlus, EPAC 2006, p.1897.
- [15] J. Qiang, R. Ryne, S. Habib, V. Decyk, J. Comp. Phys. vol. 163, 434, (2000).
- [16] J. Qiang, R. D. Ryne, M. Venturini, A. A. Zholents, I. V. Pogorelov, Phys. Rev. ST Accel. Beams, 12, 100702 (2009).
- [17] E. L. Saldin, E. A. Schneidmiller, and M. V. Yurkov, Nucl. Instrum. Methods Phys. Res., Sect. A398, 373 (1997).
- [18] M. Borland, Phys. Rev. Special Topics - Accel. Beams 4, 070701 (2001).
- [19] G. Stupakov and P. Emma, "CSR Wake for a Short Magnet in Ultrarelativistic Limit," SLAC-PUB-9242, 2002.
- [20] W. Press, S. Teukolsky, W. Vetterling, and B. Flannery, Numerical Recipes in FORTRAN, Cambridge University Press, New York, 1992.
- [21] I. Pogorelov, J. Qiang, R. D. Ryne, M. Venturini, A. Zholents, R. Warnock, in Proceedings of 9th Int. Comp. Accel. Physics Conf., p. 182, 2006.
- [22] J. Qiang, S. Lidia, R. D. Ryne, C. Limborg-Deprey, Phys. Rev. Special Topics - Accel. Beams 9, 044204, (2006).
- [23] A. Novokhatski, Phys. Rev. ST Accel. Beams 14, 060707 (2011).
- [24] A. Novokhatski and M. Sullivan, IPAC'10, TUPEB028.
- [25] A. Novokhatski, PAC'11, TUOAN1.
- [26] T. Agoh and K. Yokoya, Phys. Rev. ST Accel. Beams, 7(5):054403 (2004).
- [27] D. R. Gillingham and T. M. Antonsen, Jr, Phys. Rev. ST Accel. Beams 10, 054402 (2007).
- [28] G. V. Stupakov and I. A. Kotelnikov, Phys. Rev. ST Accel. Beams 12, 104401 (2009).
- [29] K. Oide, et al., PAC'09, MO3RAI01.
- [30] D. Zhou, Ph.D. thesis, KEK/SOKENDAI, Sep. 2011.
- [31] Stephen Wolfram, The Mathematica Book, 5th ed. (Wolfram Media, 2003).
- [32] SAD home page: <http://acc-physics.kek.jp/SAD/>
- [33] G. Bassi, J. A. Ellison, K. Heinemann, and R. Warnock, Phys. Rev. ST Accel. Beams 12, 080704 (2009).
- [34] G. Bassi, J. A. Ellison, K. Heinemann, and R. Warnock, Phys. Rev. ST Accel. Beams 13, 104403 (2010).
- [35] B. Terzic and G. Bassi, Phys. Rev. ST Accel. Beams 14, 070701 (2011).
- [36] G. Bassi, J. A. Ellison and K. Heinemann, Proceedings of ICAP09, San Francisco, September, 2009. See Jacow for ICAP09.
- [37] K. Heinemann, Two topics in particle accelerator beams: A Vlasov-Maxwell treatment of coherent synchrotron radiation and topological treatment of spin polarization, PhD dissertation, Math&Stat, University of New Mexico, May 2010. Archived on ProQuest.
- [38] B. Terzic and R. Li, PR ST-AB, in preparation, 2012.
- [39] R. Li, Nucl. Instrum. Meth. Phys. Res. A, 429:310, 1999.
- [40] R. Li, Proc. of The Second ICFA Advanced Accelerator Workshop on the Physics of High Brightness Beams, 1999.
- [41] J.-L. Vay, Phys. Rev. Lett. 98 (2007) 130405.
- [42] J.-L. Vay, C.G.R. Geddes, E. Cormier-Michel, D.P. Grote, Phys. Plasmas 18 (2011) 030701.
- [43] W. Fawley, J.-L. Vay, AIP Conf. Proc. 1086 (2009) 346.
- [44] J. L. Vay, Phys. Plasmas 15 (2008) 056701.
- [45] W.M. Fawley, J.-L. Vay, Jacow Conf. Proc. IPAC10 (2010) 1874.
- [46] D.P. Grote, A. Friedman, J.-L. Vay, and I. Haber, AIP Conf. Proc. 749 (2005), 55.